Energetic Ion-Stimulated Desorption of Physisorbed Molecules

Chad A. Meserole,[†] Erno Vandeweert,[‡] Zbigniew Postawa,[§] Brendan C. Haynie,[†] and Nicholas Winograd*[,†]

Department of Chemistry, The Pennsylvania State University, University Park, Pennsylvania 16802, Laboratorium voor Vaste-Stoffysica en Magnetisme, Celestijnenlaan 200 D, B-3001 Leuven, Belgium, and Smoluchowski Institute of Physics, Jagellonian University, ul. Reymonta 4, PL 30-059 Krakow 16, Poland

Received: April 17, 2002; In Final Form: July 23, 2002

We have conducted an experimental investigation into molecular desorption stimulated by 8 keV Ar^+ ions. The investigated systems are comprised of aromatic molecules (benzene and phenol) adsorbed to an Ag(111) surface. Resonance-enhanced laser ionization coupled with time-of-flight mass spectrometry provide the ability to obtain quantum state resolved kinetic energy distributions of the desorbed molecules. Our results indicate that the desorption mechanisms for the molecules are dictated by the molecular coverage and determine if the molecules are desorbed in an internally excited state. We use specific mechanisms observed in molecular dynamics simulations reported in the literature to describe our experimental observations. In the low coverage regime, ballistic collisions between dislocated silver substrate atoms and the adsorbed molecules lead to the emission of energetic molecules. A collision between a single substrate atom and an adsorbed molecule leads to the emission of translationally and internally hotter molecules. A collision between an adsorbed molecule and several substrate atoms with similar momentum leads to the emission of slower, internally cooler molecules. In multilayer systems, a gentler mechanism, such as a molecular collision cascade or localized heating, generates the emission of translationally slow molecules. Temperature-programmed desorption studies allow characterization of the benzene film structure and show how the emission characteristics of the desorbed molecules change concomitantly with changes in the film structure. In general, we provide a framework describing the collision events responsible for stimulated molecular desorption.

Introduction

The collision between an energetic particle and a surface initiates a complex chain of events. Following the impact, atoms, clusters of atoms, or molecules can be ejected in a variety of charge and internal energy states.[1,2] The complex interactions between an energetic particle and a solid surface have both beneficial and undesired consequences. Collision-induced erosion is detrimental in technological applications such as confining high-temperature plasmas.[1] On the other hand, technological applications such as the deposition of high quality thin films depend on these collisions.[1] Moreover, the removal of surface-bound material by energetic particles forms the basis of surface-sensitive analytical techniques such as secondary ion, secondary neutral, and fast atom bombardment mass spectrometry (SIMS, SNMS, and FAB, respectively).[2,3,4] Mass spectral detection of the secondary species gives SIMS and SNMS the ability to provide a detailed chemical analysis of molecules present on surfaces, including surfaces of biologically relevant materials.[5]

A general theory describing collisions between energetic particles and *all* types of surfaces has not been established. Sputtering of atoms from simple elemental targets is relatively well understood and described by a variety of theoretical treatments including computer simulation models or methods.[6,7] However, a scarcity of reliable experimental data prevents the development of a unifying theory governing the interaction between organic surfaces and particles having keV kinetic energy, which is the typical energy range of the probes used in desorption mass spectrometry.[3,8,9] This amount of energy is far in excess of chemical bond energies in an organic molecule.[10] It is remarkable that any intact molecules can survive and be desorbed by such high energy impact events. In an impact with a molecular surface, the energy can be transferred into translational modes, as well as rotational and vibrational modes. Understanding how the kinetic energy of the primary ion is distributed among the atoms and molecules of the target is paramount for developing a general theory. A basic understanding of the complex processes giving rise to molecular desorption has been provided by molecular dynamics computer simulations.[11] It is observed that the primary ion's kinetic energy is dissipated in the substrate. Moving substrate atoms, which have several orders of magnitude less energy than the primary ion, collide with and ultimately desorb the fragile molecules.[11]

Observing the emission characteristics of the ejected secondary particles, which can be either charged or neutral, provides the means for learning how an energetic particle interacts with a surface and how its kinetic energy is distributed. Probing neutral species has major benefits. Most of the desorbed particles are in a neutral charge state.[1,2,9] Therefore, the observations are not convoluted with the ionization process, which can be influenced by the matrix.[3,9] Finally, the experimental findings are more readily compared to theoretical models such as molecular dynamics (MD) computer simulations that cannot easily account for the ionization process.[12]

We chose to examine ion beam stimulated molecular desorption from systems of aromatic molecules adsorbed onto an

* Corresponding author: Tel.: 1-814-863-0001. Fax: 1-814-863-0618. E-mail: nxw@psu.edu.
[†] The Pennsylvania State University.
[‡] Laboratorium voor Vaste-Stoffysica en Magnetisme.
[§] Jagellonian University.

10.1021/jp0209906 CCC: $22.00
Published on Web 11/19/2002

Ag(111) surface. The system composed of benzene (C_6H_6) on an Ag(111) surface has several attributes that cause it to be a good candidate for these studies. Condensing C_6H_6 molecules on an Ag(111) surface creates a simple, binary system because silver is inert toward benzene.[13] The physisorption of benzene molecules onto Ag(111) is reversible with temperature, and a wide variety of surface coverages can be easily and reproducibly created.[13,14] We can create well-characterized submonolayer to multilayer systems. Such control is critical for isolating various phenomena and for providing experimental systems that may be accurately modeled. Finally, the ultraviolet spectroscopy of benzene is well documented[15,16] and experimentally accessible.[17,18]

Previously, desorption of benzene molecules from the C_6H_6/Ag(111) system has been studied experimentally[13] and with MD computer simulations.[19] The experiments, which utilize a nonresonant ionization scheme for detecting benzene molecules, illustrate that the desorption mechanism switches as benzene exposure is increased. In the system with a low exposure of benzene on the Ag(111) surface, collisions between substrate atoms and molecules lead to molecular ejection.[13] In high-exposure systems, the molecules are desorbed with less kinetic energy as a result of localized heating.[13] More recently, we have shown that benzene molecules can be photoionized with resonance-enhanced laser-based schemes that allow for quantum-state-resolved detection.[17,18] Obtaining quantum-state-resolved distributions of benzene molecules desorbed in the molecular ground state and in a vibrationally excited state allows us to explore in greater detail how the kinetic energy of the primary ion is distributed in the target material, permitting molecular ejection rather than fragmentation.

We have extended our previous work by applying quantum state specific detection methods to phenol molecules and by incorporating temperature-programmed desorption studies. With this model system, it is possible to identify specific desorption mechanisms that are applicable to physisorbed molecules in general. Additionally, we show that increased molecular binding energy suppresses the emission of slow molecules from approximately a monolayer system, yet readily facilitates the gentler mechanisms associated with thick multilayer systems. Temperature-programmed desorption not only permits us to verify the structure of the benzene films, but also allows us to show experimentally the dependence of the desorption mechanism on this structure.

One facet of this study is to investigate the role of binding energy in molecular desorption events. A stronger binding of the molecules to each other and to the metal substrate should cause the molecules to desorb with higher kinetic energy since a similar trend has been observed for metallic targets.[1] We chose to study phenol (C_6H_6O) molecules adsorbed to an Ag(111) surface to accomplish this goal. Phenol molecules have increased intermolecular interactions due to the hydrogen bonding through the hydroxyl group. Because of the similarity to benzene molecules, a direct comparison of the kinetic energy distributions of the two molecules to test this hypothesis is reasonable. Moreover, the UV spectroscopy of phenol is documented.[20]

A major goal of these experiments is to establish relationships between internal energy excitation pathways and molecular fragmentation so as to improve the information content of desorption mass spectrometries. The desorption of both internally excited species and secondary ions is sensitive to the local chemical environment or electronic structure of the surface.[9] Studying the emission of internally excited molecules from varying chemical environments may allow us to understand ejection mechanisms or even emission probability of molecular secondary ions from organic surfaces. The quantum-state-resolved yields and kinetic energy distributions may possibly allow physical characteristics of thin organic films, such as molecular orientation or film thickness, to be measured directly. Since the hydroxyl group participates in hydrogen bonding, a system composed of phenol molecules adsorbed to Ag(111) may yield insight into how the desorption of biomolecules, for instance, dissolved in frozen aqueous solutions may be influenced by this type of bonding.[21,22]

Theoretical treatments, especially MD simulations, can guide experiments and aid in the interpretation of experimental results. MD computer simulations are crucial for pinpointing specific mechanisms because they provide an atomic-level view of the desorption process. MD simulations based on classical mechanics have some inherent restrictions or limitations. For instance, electronic effects taking place in the collisions or ion creation events are generally beyond the scope of classical equations.[12] However, dynamic events taking place on a fast time scale, such as the collisions in a solid irradiated with keV particles, can be successfully modeled[19] as gauged by direct comparison to experiments. Under these circumstances, the MD strategy is a powerful approach for helping to unravel the experimental data at the molecular level.

In this paper molecular desorption mechanisms are shown to be coverage dependent and specific mechanisms are shown to lead to internal molecular excitation. In the low coverage regime, ballistic collisions between dislocated substrate atoms and the adsorbed molecules cause energetic molecules to desorb. A collision between a single substrate atom and an adsorbed molecule yields translationally and internally hotter molecules. A cooperative mechanism involving several substrate atoms with similar momentum leads to the emission of slower, internally cooler molecules. Gentler mechanisms, such as a molecular collision cascade or localized heating, generate the emission of translationally cooler molecules from multilayer systems.

Our results reveal that the physics and chemistry of the molecular systems are deeply interwoven and profoundly influence the energetic ion-beam-stimulated desorption of molecules. These findings can be extrapolated to more diverse molecular systems and they pave the way toward a more thorough understanding of energetic particle/solid surface interactions.

Experimental Section

The apparatus in which the experiments are conducted is described in detail elsewhere.[23] Briefly, the instrument consists of an ultrahigh vacuum (UHV) chamber (base pressure of 1×10^{-10} Torr) equipped with low-energy electron diffraction (LEED) and with laser post-ionization time-of-flight (TOF) mass spectrometry. A quadrupole mass analyzer for performing temperature-programmed desorption (TPD) experiments is also mated to the chamber. A $\sim$15 μA (continuous current) Ar^+ ion beam is modulated to produce 200 ns wide pulses that impinge the surface at 45° incidence. The pulsed ion beam accelerated to 8 keV and focused to a 3 mm spot initiates the desorption event. The accumulation of surface damage is minimized by limiting the ion dose to $\sim 10^{11}$ Ar^+/cm^2. The photoionizing laser pulses from the frequency-doubled output of an Nd:YAG-pumped tunable dye laser are focused to a ribbon shape (1 mm $\times$ 10 mm cross section) approximately 1 cm in front of the sample surface and parallel to the plane of a position-sensitive microchannel plate (MCP) detector. The laser pulses have a typical output of about 1 mJ per 6 ns pulse. The photoionized

particles are mass selectively detected on the gated MCP detector. Time-of-flight distributions, which are converted to kinetic energy distributions, of the mass-selected species, are measured by systematically varying the time delay between the ionizing laser pulse and the Ar^+ ion pulse and monitoring the signal amplitude from the particles that are emitted to $\pm 20^o$ of the surface normal.

The constituents of the experimental sample are cleaned prior to the experiment. The Ag(111) surface is sputter cleaned with several cycles of Ar^+ ion bombardment from a defocused continuous ion beam ($\sim$15 μA, 8 keV, 5 min/cycle) and annealed at 730 K for several minutes. The silver crystal is determined to be clean when a crisp LEED image is obtained. The liquid benzene sample (EM, 99%) is treated with several freeze−pump−thaw cycles to remove dissolved gaseous impurities. After cleaning the benzene sample and the Ag(111) surface, the silver crystal is cooled to 120 K, and benzene vapor is dosed into the chamber via a leak valve. The chamber is filled to a specific pressure for a specific time period to obtain a particular benzene exposure on the Ag(111) surface. Exposures are reported in Langmuir (L) units (1 L = 1×10^{-6} Torr s). Benzene molecules form a monolayer by a 5−7 L exposure[13,18] and form an ordered monolayer in a (3×3) arrangement by a 5 L exposure.[14]

Before starting the experiments involving phenol molecules, the phenol sample (Sigma, 99.0%) is cleaned. Excess nonphenol vapor from the headspace in the phenol dosing manifold is removed by rough-pumping it several times while the phenol is a solid at room temperature. After liquefying the phenol sample by heating the manifold to approximately 340 K, the manifold is once again rough vacuumed. The leak valve on the manifold is directly attached to a loadlock that is pumped by a turbo pump and that is separated from the main chamber via a gate valve. Once the silver single crystal is cooled to about 120 K, the phenol vapor is dosed into the main chamber by opening the loadlock gate valve and opening the dosing manifold leak valve. In the same manner for dosing benzene molecules, the phenol vapor is dosed at a specific pressure for a specific time, and the doses or exposures are reported in Langmuir (L) units.

Secondary neutral time-of-flight mass spectrometry is the tool that enables us to study ion-beam-stimulated molecular desorption. Background-corrected secondary neutral TOF mass spectra of both the benzene/Ag(111) system and the phenol/Ag(111) system are illustrated in Figure 1. The peak-normalized mass spectra of the clean Ag(111) substrate prior to dosing (0 L) and spectra after dosing a 20 L exposure of the molecules showcase the prominent features typically observed. The peaks at *m*/*z* 108 (Ag) and 216 (Ag_2) emanate from the substrate and rapidly attenuate with increased exposures of the organic molecules. The peak height ratios of Ag/Ag_2 are different in Figure 1A and 1B because of the wavelength-dependent nature of the photoionization process. The 0 L spectra are recorded with 266.8 and 275.1 nm laser radiation in Figure 1A and 1B, respectively. We find that 275.1 nm laser radiation readily facilitates Ag_2 ionization; hence, the Ag_2 peak appears very large in Figure 1B. After dosing, the prominent peaks from the organic species are the molecular photoion peaks at *m*/*z* 78 and 94 for C_6H_6 and C_6H_5OH, respectively. A C_4H_X fragment is observed in the benzene spectrum, and a benzenoid fragment is present in the phenol spectrum. These fragments are largely the result of photofragmentation, as they are present in the gas-phase mass spectra. Moreover, they have TOF distributions that are identical to the parent photoion. Although it appears that the low mass wing of the Ag peak may be an isobaric interference for the phenol molecules in the TOF measurements, it actually provides an insignificant amount of interference. TOF distributions of *m*/*z* 94 were measured before dosing any phenol on the Ag(111). The yield from this measurement makes up 0.3% of the total yield from an identical measurement after a 1 L exposure of phenol to the Ag(111) surface.

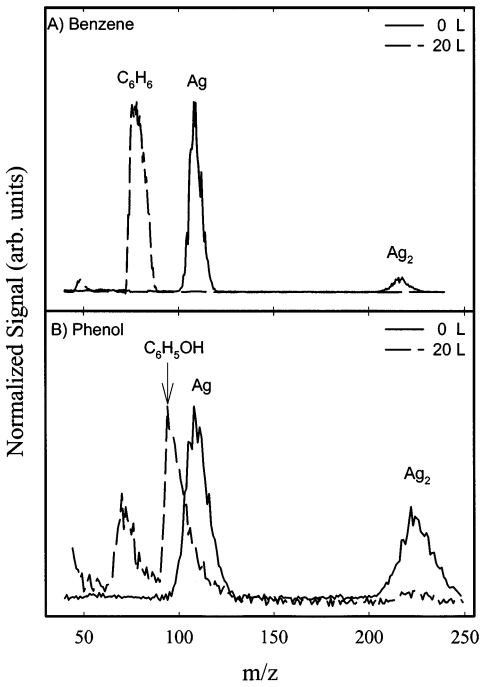

Figure 1. Secondary neutral time-of-flight mass spectra. The top panel (A) represents mass spectra from the benzene/Ag(111). The bottom panel (B) represents spectra from the phenol/Ag(111). Plots labeled 0 L are the mass spectra of the clean silver substrate prior to dosing the aromatic molecules. The mass spectra of the sample that is exposed to 20 L of the aromatic molecules is obtained with the laser tuned for probing the ground-state organic molecules.

Resonance-enhanced ionization provides the means to probe specific quantum states of benzene molecules and phenol molecules. The one-color two-photon ionization ultraviolet (UV) spectrum of benzene vapor is illustrated in Figure 2A. The spectrum is created by leaking the benzene vapor into the chamber at a rate such that the pressure is constant at 1.4×10^{-9} Torr and recording the mass spectral signal of the molecular photoion (*m*/*z* 78) as the wavelength of the laser output is scanned. The ionization spectrum is very similar to the UV absorption spectrum obtained by Callomon and coworkers.[15] The peaks labeled as 6_0^1 ($\sim$259.0 nm) and 6_1^0 ($\sim$266.8 nm) mark the transitions of interest. Ground-state benzene molecules (C_6H_6) are ionized by first pumping the 6_0^1 transition originating from the zero vibrational level of the molecular ground state[15] (C_6H_6) with a 259.0 nm photon and absorbing a second 259.0 nm photon provides the ionization.[17,18] Vibrationally excited benzene molecules (C_6H_6*) are ionized by first pumping the 6_1^0 transition starting from the first vibrationally excited state of the ν_6'' mode, lying $\sim$0.1 eV above the molecular ground-state level,[15] with a 266.8 nm photon and absorbing a second photon (266.8 nm) produces the ionization.[17,18] The notation of C_6H_6 and of C_6H_6* shall be reserved for the two particular quantum states discussed above.

We have recorded a one-color two-photon ultraviolet photoionization spectrum of phenol vapor (Figure 2B) in order to determine which frequency yields adequate resonance-enhanced ionization. The spectrum is created by leaking phenol vapor into the chamber at a rate such that the chamber pressure is

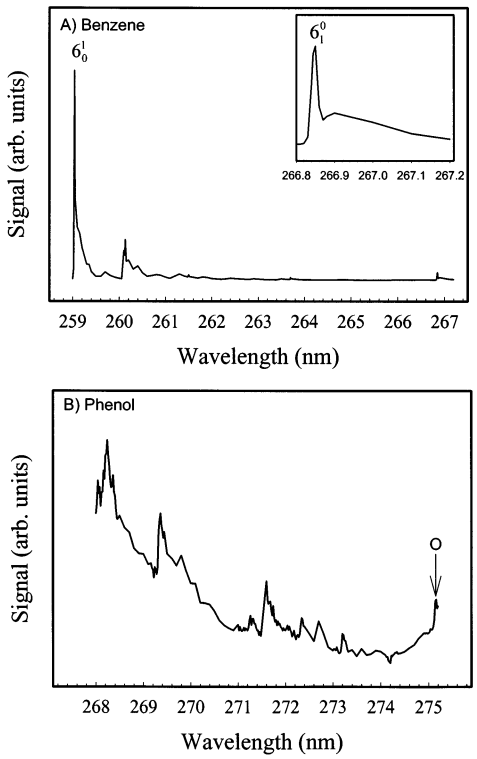

Figure 2. Ultraviolet multilphoton ionization spectra of (A) benzene and (B) phenol vapor. The inset in panel (A) is an expanded view of the peak produced by ionizing vibrationally excited benzene molecules. The label "O" in (B) corresponds to the resonant transition from the ground state to the lowest level of the first excited singlet state in phenol molecules.

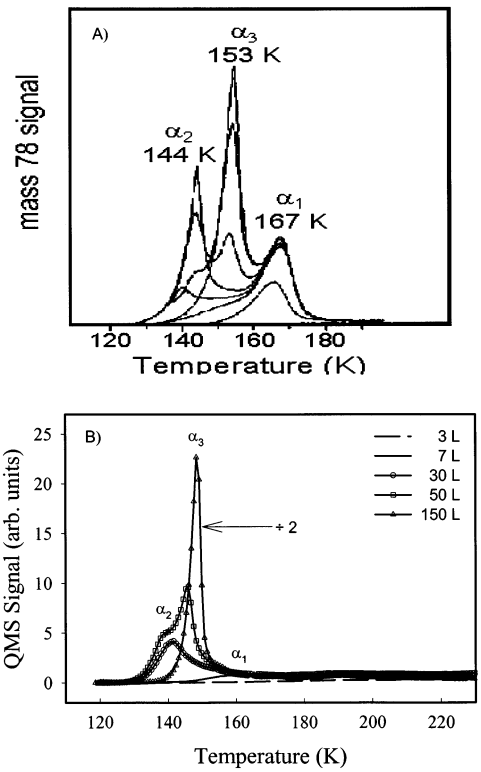

Figure 3. TPD spectra of benzene (*m*/*z* 78) desorbed from a Ru(001) substrate (A) and an Ag(111) substrate (B). Peaks that appear in the α_1 region are the result of the desorption of a monolayer or less of benzene. Peaks that appear in the α_2 region represent desorption from an intermediate metastable monolayer of benzene. Desorption peaks that appear in the α_3 region are from the desorption of bulk multilayers of benzene. The signal from the 150 L exposure in panel (B) has been divided by 2. (Figure 3A is reproduced from ref 26 with permission from Elsevier.)

held constant at 1.4×10^{-9} Torr and collecting the mass spectral signal of the molecular photoion (*m*/*z* 94).

Transitions occurring in the ultraviolet spectrum of phenol have been listed in the literature.[20] In the UV absorption spectrum of phenol, the origin of the band observed around 275 nm is reported to occur at 36351.9 cm^{-1} (275.09 nm).[20] It has also been reported to be at 36348.7 cm^{-1} (275.11 nm),[24,25] which is in better agreement with our findings (275.14 nm). The corresponding transition in the photoionization spectrum is labeled as "O" in Figure 2B. This transition pumps the ground-state molecules into the lowest level of the first excited singlet electronic state.[20] Absorbing a second photon at this wavelength produces the photoionization. Ground-state phenol molecules can be probed more efficiently with 268.2 nm radiation than with 275.1 nm radiation. However, the 268.2 nm radiation is not as sensitive a probe as 275.1 nm radiation for nonresonantly ionizing silver monomers and dimers. Therefore, 275.1 nm laser output is selected for these experiments. Unfortunately, there are no spectral lines within range of available laser wavelengths which allow vibrationally excited phenol molecules to be detected.

Temperature-programmed desorption experiments of benzene adsorbed on the Ag(111) surface are performed by heating the crystal and simultaneously monitoring the crystal surface temperature and the molecular ion peak amplitude generated by the quadrupole mass analyzer. The silver crystal is heated from the backside by electron bombardment; however, the temperature of the front side of the crystal is monitored. The front side of the crystal is in line-of-sight of the ionizer and is located approximately 2 cm away from the quadrupole entrance aperture. The crystal is heated at approximately 0.8 K/s up to about 160 K and at 0.4 K/s for temperatures greater than 160 K.

Results and Discussion

The structure of benzene overlayers created by various exposures is characterized by several different phases. In a complete monolayer, the benzene rings lie parallel to the substrate surface.[14,26,77] This molecular orientation is designated as the α_1 phase.[26,27] As more benzene molecules condense onto the surface, the α_1 phase saturates and some molecules tilt from the surface. This tilting is the beginning of the α_2 phase.[27] After the α_2 phase saturates, a bulk crystalline phase, α_3, grows.[27] The molecular orientation in the bulk α_3 phase is such that the planes of the benzene rings are perpendicular to each other, generating a herringbone-like structure. The molecules in the layer nearest the substrate are tilted from the surface.

To elucidate the structure of our various benzene overlayers, we have performed TPD experiments to compare our results with those of Jakob and Menzel.[26,27] Their experiments are based on a Ru(001) substrate, to which benzene first chemisorbs.[26,27] However, in their experiments, the discussion of phases and overlayer structures is limited to benzene layers physisorbed on the chemisorbed benzene layer. Therefore, their observations should be applicable to our results because the benzene molecules in all our benzene/Ag(111) systems are physisorbed. TPD spectra of benzene molecules emitted from a Ru(001) surface and from an Ag(111) surface are given in Figure 3. Our results from the benzene/Ag(111) system are qualitatively similar to the data in ref 26 (Figure 3A), suggesting a very similar behavior for the C_6H_6/Ag(111) system. The α_1, α_2, and α_3 phases are reported to have TPD peaks at 165, 142, and 152 K, respectively, after correcting for the effect of readsorption.[26]

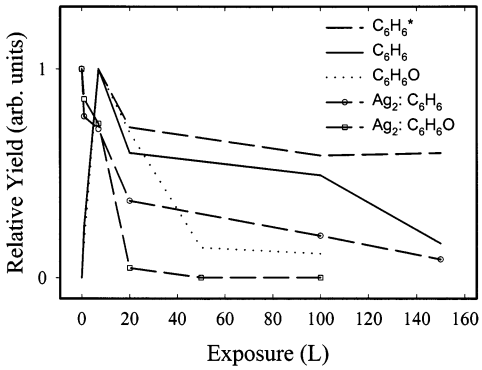

Figure 4. Relative yields as a function of exposure. The lines without symbols are for the yields of the organic species from the molecular overlayer (C_6H_6* = dashed; C_6H_6 = solid; C_6H_6O = dotted). The yields of the organic species are normalized to the maximum observed yield, which occurs at 7 L. The lines with open symbols are the relative yields of the substrate species (silver dimers), which are normalized to the yields from a clean Ag(111) surface (0 L) prior to dosing the molecules. The open circles represent data from benzene experiments. The open squares represent data from phenol experiments.

We observe that the α_1 phase is formed by exposures less than 7 L (Figure 3B). An exposure of 7 L yields a peak at 158 K. In this case, most of the molecules are in the α_1 phase, but some are transitioning to the α_2 phase. As a result, the molecular overlayer created by a 7 L exposure is more densely packed than the (3×3) arrangement. The α_2 phase is saturated at 30 L (142 K). Both the α_2 and α_3 phases are present in exposures greater than 30 L and up to 50 L. Only the α_3 phase is present in exposures greater than or equal to 100 L. In our TPD spectra, the peaks at temperatures greater than 165 K are due to desorption from other parts of the instrument.

Phenol molecules adsorbed on an Ag(111) surface are not as thoroughly studied as benzene molecules on an Ag(111) surface, and as a result not much is known about the surface chemistry of the phenol/Ag(111) system. Because phenol molecules are both benzene-like and alcohol-like, knowledge of the surface chemistry present on silver surfaces for both alcohols and benzene should be applicable to understanding the surface chemistry present in a phenol/Ag system. Benzene[13,14] and some alcohols[28] adsorb onto silver without the formation of strong bonds between the molecules and the silver surface. Moreover, for certain surface concentration conditions the benzene molecules[14] and the alcohol molecules[28] lie parallel to the silver surface. In addition, phenol is known to reversibly adsorb to a silver surface without dissociating.[29] Therefore, we conclude that a monolayer of phenol molecules on an Ag(111) surface is constructed such that the ring of the molecules is parallel to the silver surface. Moreover, the phenol molecules are intact and do not have strong chemical bonds to the silver surface. Like multilayers of benzene molecules, the bulk phenol structure is different from the structure of a monolayer on the crystal surface.[29] Unfortunately, TPD results of the phenol/Ag(111) system yielded only a single peak at all exposures, and we were unable to discern any useful information regarding film structure or possible orientation phases.

In characterizing the desorption of species from surfaces irradiated by energetic particles, a particularly useful quantity is the yield. The yield is obtained by integrating the time-of-flight or kinetic energy distributions of the particles emitted $\pm 20°$ from the surface normal. The relative yields of the species relevant to this study are plotted as a function of molecular exposure in Figure 4. Each plot is normalized to the maximum value in the series. The yields of the substrate species, as represented by the silver dimers (Ag_2), are greatest from the clean silver crystal with no molecular adsorbates present. It should be pointed out that all Ag_2 yields measured in the benzene experiments are the result of ionizing with 266.8 nm laser radiation and that all Ag_2 yields measured in the phenol experiments are the result of ionizing with 275.1 nm laser radiation. In this way, ionization cross section effects within each series are eliminated and the relative yields reflect the true behavior within each set of experiments. The yield of the dimers tends to decrease rapidly for exposures up to 20 L. For exposures greater than 20 L, the decrease in the Ag_2 emission is less dramatic. It is reasonable to suspect that blocking of the substrate species by the molecular overlayer is the main culprit for the yield suppression. However, in systems with multilayers of adsorbate molecules, an additional means of yield reduction may be in operation. As the primary ion passes through the molecular overlayer, it may lose energy to the overlayer. The kinetic energy loss can negatively affect the primary ion's sputter yield.[1,3] However, the extent of the primary ion kinetic energy reduction by these molecular overlayers is currently not known and can only be ascertained by more detailed studies.

The yield of the intact aromatic molecules desorbed from the molecular overlayer exhibits a much different trend than that of the substrate species. The yield of molecules increases for exposures up to 7 L, but declines slowly as the amount of benzene is increased further. An exposure of 7 L approximately creates a monolayer of benzene molecules on the Ag(111) surface. This yield effect has been reported previously for various molecules.[13,30] Molecular dynamics simulations suggest that the reason for this behavior is that the target looks more like carbon with respect to the energetic ion beam.[13] This lighter material is less efficient at redirecting the momentum of the incident particle and inducing molecular desorption.[12]

The yield of phenol molecules also exhibits a maximum as a function of exposure as shown in Figure 4. On a per Langmuir basis, phenol is more efficient than benzene at suppressing the silver dimer emission. For example, a 20 L exposure of benzene reduces the dimer yield to ~37% compared to a clean silver substrate. A 20 L exposure of phenol reduces the dimer yield to ~5% of that from a clean substrate. At this point, we speculate that the reason for this effect is that the sticking probability of phenol is higher than that of benzene resulting in a thicker film for an equivalent exposure.

The shapes of the kinetic energy distributions of the desorbed ground-state phenol molecules are similar to those of ground-state benzene molecules (Figure 5). It is interesting to compare the shapes of these distributions to an exponential function such as a Maxwell−Boltzmann distribution and to a polynomial distribution such as the Thompson distribution.[31] The ground-state benzene molecules and the ground-state phenol molecules are best fit by an exponential distribution with an effective temperature of 2276 and 5996 K, respectively, while the excited-state distribution of benzene is best fit by a Thompson distribution with surface binding energy of 0.45 eV. This approach to data analysis is not very satisfactory, however, because these shapes are known to be perturbed by preferential dissociation of the high kinetic energy molecules and because the concept of temperature in this time regime is highly questionable. Moreover, the Thompson equation itself was not developed to describe molecular overlayers. Although it is not physically very meaningful to extract parameters from these distributions for molecular systems, it is interesting to examine the fits for common features and trends.

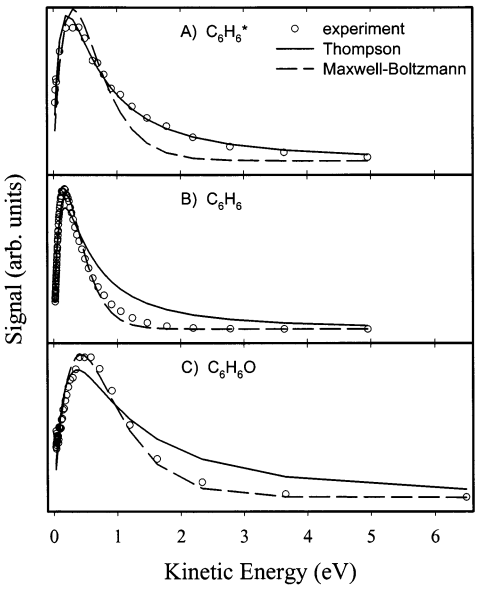

Figure 5. Kinetic energy distributions of molecules desorbed from an Ag(111) surface. These data are obtained from a 7 L exposure of benzene (A and B) and of phenol (C). The distribution of vibrationally excited benzene molecules is illustrated in (A), whereas molecules in the ground state are shown in (B). The data are fitted with a Maxwell−Boltzmann formula and with a Thompson formula. The Maxwell−Boltzmann formula is given by $Y(E) = c \times E \times \exp[-E/kT]$, where c, a proportionality constant, and T, temperature, are fit parameters. The values for T are 3644, 2276, and 5996 K, respectively. The Thompson formula is given by $Y(E) = A \times E \times (U + E)^{-3}$, where A, a proportionality constant, and U, surface binding energy, are fit parameters. The values for U are 0.45, 0.36, and 0.92 eV, respectively.

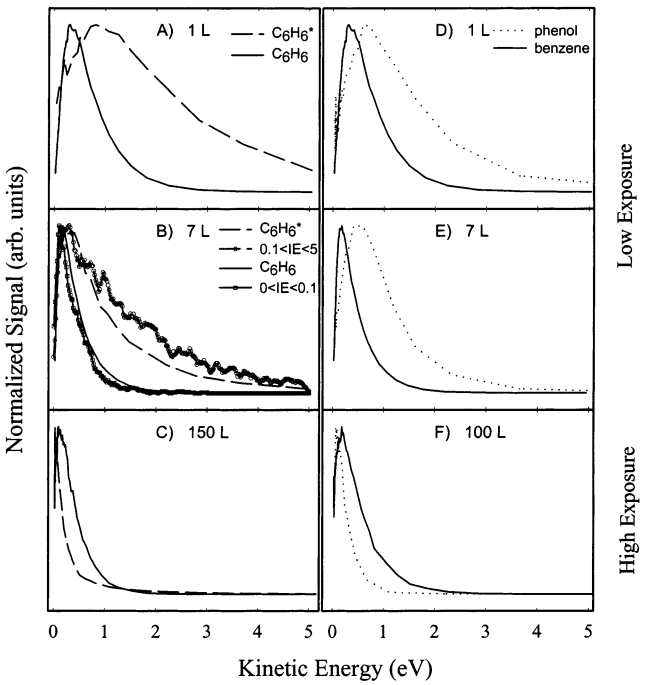

Figure 6. Kinetic energy distributions of molecules desorbed from Ag(111) by an energetic ion beam. Kinetic energy distributions of ground-state and vibrationally excited benzene molecules are shown with solid and dashed lines, respectively. Kinetic energy distributions of phenol molecules desorbed in the molecular ground state are shown with dotted lines. Kinetic energy distributions from MD simulations of the benzene/Ag(111) system are illustrated in panel (B) for comparison to experiment. The distribution of the internally cool molecules is shown as a dashed line with open circles. The distribution of the internally hot molecules is shown as a dashed line with open squares.

The quantum state resolved kinetic energy distributions of benzene and phenol desorbed from overlayers created by various exposures are compared in Figure 6. In the low coverage regime (1 and 7 L), where most of the molecules are lying parallel to the Ag(111) surface, a ballistic mechanism is proposed to be responsible for the desorption of the benzene molecules,[12,19] a conclusion based largely on MD simulations. Moreover, a thermal or evaporative mechanism is ruled out because the most probable kinetic energy of even the translationally slowest molecules is on the order of several thousand Kelvin, yet the surface temperature is 120 K. It is interesting to note that the kinetic energy distributions of the C_6H_6* molecules and the C_6H_6 molecules differ. Specifically, the C_6H_6* molecules (dashed line) are translationally faster than the C_6H_6 molecules (solid line). Although MD calculations suggest that ballistic mechanisms are responsible for the desorption of both types of molecules, there are different types of ballistic collisions that cause the emission of the C_6H_6* molecules and the C_6H_6 molecules.[12,19]

Data from MD simulations of 5 keV Ar bombardment of a benzene/Ag(111) system similar to a system created experimentally by a 7 L exposure are plotted in Figure 6B. These data are taken from a set of MD simulations performed to examine the behavior of desorbed metal atoms as a function of molecular overlayer coverage.[32] Excellent agreement between the MD simulations and experimental results of ground-state silver atom emission is achieved. The kinetic energy distribution of molecules with little or no internal excitation (solid line, open squares) agrees well with the distribution of the experimentally detected ground-state molecules (solid line). There is also good agreement between the kinetic energy distribution of the internally excited molecules (dashed line, open circles) and the distribution of the vibrationally excited molecules detected experimentally (dashed line). Since C_6H_6* lies ∼0.1 eV above the ground state, 0.1 eV is used as an internal energy upper limit of the molecules to be compared to the ground-state molecules of the experiment. Molecules in the MD simulations with internal energies ranging from 0.1 to 5 eV are compared to the experimentally detected excited-state molecules. An upper limit of 5 eV is selected because molecules with larger amounts of internal energy may decompose on the way to the detector and would not be observed experimentally. In fact, signal loss due to molecular decomposition has been invoked to explain why the high energy tail of the experimentally measured kinetic energy distributions tends to fall off more rapidly than the tails of energy distributions from the MD simulations.[12,19]

Because of the success of the modeling of energetic ion/solid surface interactions and agreement with experiment, we believe that the molecular level picture provided by the MD simulations is extremely valuable. The simulations reveal that benzene molecules cannot survive a direct impact with the incident projectile, and as a result this type of interaction is not playing a significant role in the desorption of intact molecules.[19] MD simulations reveal that a collision between a fast silver monomer and a benzene molecule desorbs a translationally energetic molecule that is internally excited.[19] This type of collision is depicted in Figure 7A. Such collisions not only impart sufficient kinetic energy to cause the desorption of the molecules, but also stretch bonds, distorting the molecule. Thus, these types of collisions provide a means of internal excitation. Collisions between an adsorbed molecule and several Ag atoms with similar momentum cooperatively liftoff, internally cool molecules.[19,33,34] A similar rendering of the cooperative process is presented in Figure 7B. As illustrated in Figure 7B, this type of ballistic collision gently pushes the benzene molecule with

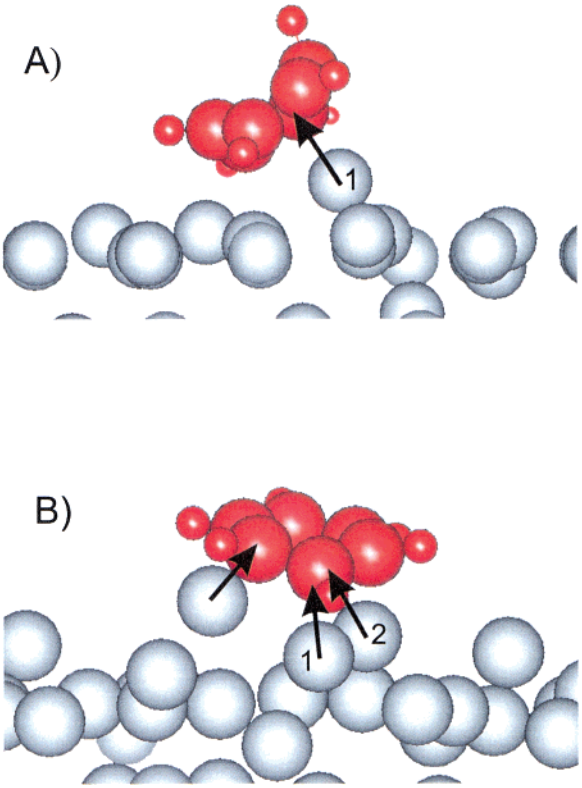

Figure 7. Illustrations of molecular desorption mechanisms. These illustrations represent systems comprised of a monolayer or less of benzene molecules (red) physisorbed to a metal surface (gray). The emission of internally and translationally hot molecules is depicted in (A). The desorption of molecules in the ground state is represented in (B).

little or no internal perturbation into the vacuum. Because benzene and phenol have kinetic energy distributions of similar shapes, we conclude that the collision scenarios observed in MD simulations for benzene are applicable to a broader class of physisorbed molecules.

The kinetic energy distributions of benzene and phenol molecules appreciably shift toward lower energy values as the exposure is increased. There are at least three reasons for this shift. Results from MD simulations using an atomic adsorbate overlayer of mass 78 suggest that the shift is due to an enhanced number of collisions between adsorbate atoms as more atoms are placed on the surface.[19] Moreover, theoretical calculations show that as the number of benzene molecules lying parallel to an Ag(111) surface increases, the binding energy of the benzene molecules to the surface decreases.[31] As more molecules are crowded onto the surface, some of them tilt away from the surface, which is associated with the appearance of the α_2 phase. When the molecules tilt, the average binding energy of the molecules to the surface decreases. Our TPD results verify the presence of this trend. The desorption temperature shifts from ~165 K to ~142 K as the benzene overlayer structure changes from α_1 to α_2. As a consequence, a crowded surface leads to the desorption of an increased number of slower molecules. The MD studies have also shown that the orientation of molecules on the metal surface plays a key role in the desorption of the molecule via collisions with substrate atoms.[32] Molecules oriented perpendicular to the surface are more susceptible to dissociation. This orientation effect could lead to increased numbers of translationally energetic benzene molecules in highly excited states that dissociate before detection. Therefore, the high energy tail of the kinetic energy distribution will fall off even more rapidly as the surface become more crowded with molecules.

Some differences between the emission characteristics of the ground-state molecules from the two systems exist. Notably, the ground-state phenol molecules desorbed from a low exposure system are more energetic than ground-state benzene molecules desorbed from a surface subjected to the same exposure (Figure 6D,E). The higher kinetic energy is probably due to an increased binding energy of phenol molecules compared to benzene molecules as a result of the presence of lone pairs of electrons around the oxygen atom that can interact with the metal substrate.[29] Moreover, the oxygen atom in a phenol molecule acts as one more surface contact point that is not present for benzene. Finally, as the surface becomes more crowded with phenol molecules, hydrogen bonding interactions become important, stabilizing the film.

The high coverage regime is exemplified by exposures ≥ 100 L. At these exposures multilayers of phenol molecules are present and multilayers of benzene molecules are formed in the α_3 phase. These systems are more complex than the one presented by the low coverage regime. In fact, we believe there are several desorption mechanisms in operation for this complicated case as discussed below.

The emission of the C_6H_6* molecules behaves quite differently than the emission of C_6H_6 molecules. As the coverage is increased, the peak in the energy distribution shifts to lower values. In the high coverage regime, the kinetic energy distribution of the C_6H_6* molecules peaks at 0.03 eV, whereas the kinetic energy distribution of the C_6H_6 molecules peaks at 0.1 eV. Additionally, the kinetic energy distribution of the C_6H_6* molecules decays more rapidly. Both observations provide strong evidence that a different mechanism is dominant for the emission of C_6H_6* molecules.

The kinetic energy distribution of the C_6H_6* molecules indicates that the desorption mechanism involves very little energy in a given volume flowing toward the surface because the C_6H_6* molecules are not very translationally energetic. Several possible scenarios can lead to such mechanisms. The impact of the primary ion can initiate a molecular collision cascade, either directly or indirectly. As the primary ion progresses through the molecular matrix, it loses kinetic energy in collisions with molecules and can produce molecular fragments.[13,19] Fragmented molecules can collide with other molecules in the benzene overlayer and initiate the molecular collision cascade as well. Additionally, the lower binding energy of the molecules in the molecular overlayer can lead to a denser cascade resulting in the nonlinear behavior observed in elemental targets.[35] The nonlinear effects produce the emission of many particles with low kinetic energy. At the moment, not much is known about these effects, although preliminary MD simulations of ion bombardment of thick organic samples have revealed the presence of reactive organic fragments as well as cascade-like features in the organic solid.[36]

The fragments created by the impact of the primary ion will certainly react with other intact molecules or with other fragments, releasing thermal energy. These exothermic reactions taking place in pockets of the poorly conducting organic overlayer can cause localized heating. This scenario has been proposed to explain the emission of slow benzene molecules from thick organic films.[13] Additionally, Pedrys and co-workers argued that localized heating due to exothermic recombination reactions taking place in an ion beam-irradiated matrix of frozen

methane are responsible for the emission of molecules with thermal kinetic energy.[37]

The kinetic energy distribution of the C_6H_6 molecules desorbed from the high coverage system is similar to, albeit somewhat narrower than, the kinetic energy distribution of the C_6H_6 molecules desorbed from the low coverage system. This similarity is presumably due to a still-present ballistic component. The presence of the ballistic component implies that some molecules are coming from deeper within the matrix. Preliminary results with benzene molecules sandwiched between an sBA layer and the Ag(111) surface show this to be the case as well.[38] However, as these molecules are in the process of desorbing, collisions with other molecules remove some of the molecules' kinetic energy. Therefore, the kinetic energy distribution of the C_6H_6 molecules is narrower than the kinetic energy distribution of the C_6H_6 molecules from the low coverage regime. Additionally, other mechanisms as discussed for the C_6H_6* desorption can be taking place. These additional channels of molecular desorption can increase the number of desorbed slow molecules, causing the kinetic energy distribution to become narrower.

The ground-state phenol molecules are less energetic than the ground-state benzene molecules desorbed from the thickest films (Figure 6F). Hydrogen bonding allows the phenol molecules to make a more strongly held together molecular matrix. For instance, the heat of sublimation is ~0.7 eV for phenol[29] and is ~0.45 eV for benzene.[26] Hence, it is reasonable to suppose that, on a Langmuir-for-Langmuir basis, more phenol molecules will be deposited on the surface. For example, as noted earlier, the phenol layer is far more efficient at suppressing the yield of the dimers. We suppose that the primary ion may deposit more of its energy in a phenol matrix than a benzene matrix made by the same exposure. If the Ar^+ ion loses its kinetic energy to the molecular matrix, then it will not be able to penetrate into the silver substrate and subsequently dislocate an appreciable amount of silver atoms. As a result, energetic interactions between silver atoms and the molecules are substantially minimized. Also, if all the energy of the incident projectile is deposited into the molecular layer alone, then more molecular fragmentation can result. The moving fragments can generate a lower energy collision cascade or generate more of a thermal mechanism via exothermic reactions. Preliminary results from MD studies[36] and related experiments[13] indicate that fragments are observed to play a role in emission of species from thick organic solids. The net result of these scenarios coupled with the absence of a contribution from ballistic collisions with substrate atoms is that the phenol energy distributions will appear narrower, especially compared to ground-state benzene from a comparable exposure.

Conclusions

We have conducted an experimental investigation into ion beam stimulated desorption of molecules. The studied systems are composed of aromatic molecules (benzene and phenol) physisorbed to an Ag(111) surface. Utilizing resonance-enhanced ionization allows us to probe molecules desorbed in specific quantum states. Probing specific quantum states provides the opportunity to garner an unprecedented level of insight into the molecular desorption process.

In systems where approximately a monolayer or less of molecules is present on the Ag(111) surface, a ballistic process involving collisions between silver substrate atoms and the molecules causes the molecular desorption. Our results indicate that ground-state molecules are desorbed as a result of a cooperative liftoff process involving collisions with several silver atoms having similar momentum. This gentle process results in translationally and internally cooler molecules ejected into the vacuum. A ballistic collision between a single swift silver atom and molecule leads to the ejection of a fast, internally excited molecule. At low coverage, internally excited molecules have more average kinetic energy than the molecules in the molecular ground state.

As the system is comprised of multilayers of molecules, the ballistic emission component becomes less dominant. Other gentler mechanisms yield translationally cooler molecules. Likely mechanistic candidates for desorbing slow molecules are a molecular collision cascade or a thermal mechanism due to localized heating. Additionally, it will be interesting to explore the notion that vibrationally excited-state molecules must be originally located near the surface/vacuum interface.

Increased binding energy of the molecules affects desorption from low exposure and high exposure systems. The higher binding strength suppresses the emission of slower molecules from the low exposure regime. As a result, ground-state phenol molecules are desorbed with higher average kinetic energy than the ground-state benzene molecules.

In terms of ion-beam-stimulated desorption of molecules from a monolayer or less of molecules physisorbed to a metal substrate, the primary function of the substrate is re-directing the momentum of the primary ion. After the impact of the incident ion, some of the primary ion's momentum is directed toward the surface/vacuum interface in the guise of moving substrate atoms. When the moving substrate atoms collide with molecules physisorbed to the substrate surface, the molecules can be desorbed into the vacuum. Because the substrate atom/physisorbed molecule collisions involve energies several orders of magnitude smaller than primary ion/adsorbed molecule collisions, *intact* molecules may be lifted from the surface. The momentum and number of substrate atoms colliding with the adsorbed molecules determines the average kinetic energy and degree of internal perturbation of the desorbed molecules. Ion-beam-stimulated desorption of molecules from bulk molecular systems can result from localized heating or molecular collision cascades. Desorbed molecules detected in an internally excited state must originate from the surface of the bulk molecular systems, whereas molecules detected in the ground state may originate from deeper in the molecular matrix.

Our experimental findings in concert with MD simulations reveal a wealth of knowledge regarding energetic particle/solid surface interactions. In particular, incorporating temperature-programmed desorption experiments has permitted us to show how the molecular film structure can change the molecular desorption characteristics. Internal energy-resolved kinetic energy distributions, coupled with mass spectra may provide an extremely powerful method of simultaneously analyzing the chemical composition and physical characteristics, such as thickness and molecular orientation, of thin molecular films.

Acknowledgment. The financial support from the National Institutes of Health, the National Science Foundation, and the Office of Naval Research, as well as the Polish Committee for Scientific Research Fund, ACK CYFRONET, and Cooperation Program between Flanders and Poland are gratefully acknowledged. E. Vandeweert is a postdoctoral fellow of the Fund for Scientific Research-Flanders (Belgium). The authors also thank B. J. Garrison, K. Krantzman, and A. Delcorte for helpful discussions.

References and Notes

(1) *Topics in Applied Physics, Vol. 64; Sputtering by Particle Bombardment III*; Behrisch, R., Wittmaack, K., Eds.; Springer-Verlag: New York, 1991.

(2) *Practical Surface Analysis, Vol 2: Ion and Neutral Spectroscopy*; Briggs, D., Seah, M. P., Eds.; John Wiley and Sons: New York, 1992.

(3) Benninghoven, A.; Rudenauer, F. G.; Werner, H. W. *Secondary Ion Mass Spectrometry*; Wiley-Interscience: New York, 1987.

(4) *Desorption Mass Spectrometry*; Lyon, P. A., Ed.; American Chemical Society: Washington, DC, 1985.

(5) Pacholski, M. L.; Cannon, D. M., Jr.; Ewing, A. G.; Winograd, N. *J. Am. Chem. Soc*. **1999**, *121*, 4716.

(6) Rosencrance, S. W.; Winograd, N.; Garrison, B. J.; Postawa, Z. *Phys. Rev. B* **1996**, *53*, 2378.

(7) Harrison, D. E., Jr. *CRC Crit. Rev. Solid State Mater. Sci.* **1988**, *14*, S1.

(8) Benninghoven, A.; Hagenoff, B.; Niehuis, E. *Anal. Chem.* **1993**, *65*, 630A.

(9) Winograd, N. *Anal. Chem.* **1993**, *65*, 622A.

(10) Carey, F. A. *Organic Chemistry*, 2nd ed.; McGraw-Hill: New York, 1992.

(11) Garrison, B. J. *J. Am. Chem. Soc.* **1980**, *102*, 6553.

(12) Garrison, B. J.; Delcorte, A.; Krantzman, K. D. *Acc. Chem. Res.* **2000**, *33*, 69.

(13) Chatterjee, R.; Riederer, D. E.; Postawa, Z.; Winograd, N. *J. Phys. Chem. B* **1998**, *102*, 4176.

(14) Dudde, R.; Frank, K. H.; Koch, E. E. *Surf. Sci.* **1990**, *225*, 267.

(15) Callomon, J. H.; Dunn, T. M.; Mills, I. M. *Philos. Trans. R. Proc. London* **1966**, *259A*, 499.

(16) Atkinson, G. H.; Parmenter, C. S. *J. Mol. Spectrosc*. **1978**, *73*, 20.

(17) Meserole, C. A.; Vandeweert, E.; Chatterjee, R.; Chakraborty, B. R.; Garrison, B. J.; Winograd, N.; Postawa, Z. *AIP Conf. Proc.* **1998**, *454*, 210.

(18) Vandeweert, E.; Meserole, C. A.; Sostarecz, A.; Dou, Y.; Winograd, N.; Postawa, Z. *Nucl. Instrum. Methods Phys. Res. B* **2000**, *164*−*165*, 820.

(19) Chatterjee, R.; Postawa, Z.; Winograd, N.; Garrison, B. J. *J. Phys. Chem. B* **1999**, *103*, 151.

(20) Bist, H. D.; Brand, J. C. D.; Williams, D. R. *J. Mol. Spectrosc.* **1967**, *21*, 76.

(21) Brown, T.; LeMay, H. E., Jr.; Bursten, B. E. *Chemistry*, 5th ed.; Prentice Hall: Englewood Cliffs, NJ, 1991.

(22) Remer, L. C.; Jensen, J. H. *J. Phys. Chem. A* **2000**, *104*, 9266.

(23) Kobrin, P. H.; Schick, G. A.; Baxter, J. P.; Winograd, N. *Rev. Sci. Instrum.* **1986**, *57*, 1354.

(24) Martinez, S. J., III; Alfano, J. C.; Levy, D. H. *J. Mol. Spectrosc.* **1992**, *152*, 80.

(25) Berden, G.; Meerts, W. L.; Schmitt, M.; Kleinermanns, K. *J. Chem. Phys.* **1996**, *104*, 972.

(26) Jakob, P.; Menzel, D. *Surf. Sci.* **1989**, *220*, 70.

(27) Jakob, P.; Menzel, D. *J. Chem. Phys.* **1996**, *105*, 3838.

(28) Zhang, R.; Gellman, A. J. *J. Phys. Chem.* **1991**, *95*, 7433.

(29) Lee, J.; Ryu, S.; Kim, S. K. *Surf. Sci.* **2001**, *481*, 163.

(30) Mollers, R.; Schnieders, A.; Kortenbruck, G.; Benninghoven, A. *Second. Ion Mass Spectrom.* **1995**, *10*, 943.

(31) Anderson, A. B.; McDevitt, M. R.; Urbach, F. L. *Surf. Sci.* **1984**, *146*, 80.

(32) Garrison, B. J. *J. Am. Chem. Soc.* **1982**, *104*, 6221.

(33) Delcorte, A.; Vanden Eynde, X.; Bertrand, P.; Vickerman, J. C.; Garrison, B. J. *J. Phys. Chem. B* **2000**, *104*, 2673.

(34) Delcorte, A.; Garrison, B. J. *J. Phys. Chem. B* **2000**, *104*, 6785.

(35) Pedrys, R. *Nucl. Instrum. Methods Phys. Res. B* **1990**, *48*, 525.

(36) Krantzman, K. D.; Postawa, Z.; Garrison, B. J.; Winograd, N.; Stuart, S. J.; Harrison, J. A. *Nucl. Instrum. Methods Phys. Res. B* **2001**, *180*, 159.

(37) Pedrys, R.; Oostra, D. J.; Haring, R. A.; Calcagno, L.; Haring, A.; de Vries, A. E. *Nucl. Instrum. Methods Phys. Res. B* **1986**, *17*, 15.

(38) Meserole, C. A.; Vandeweert, E.; Chatterjee, R.; Sostarecz, A.; Garrison, B. J.; Winograd, N.; Postawa, Z. *Second. Ion Mass Spectrom.* **1999**, *12*, 32.